Cellulose (2019) 26:8135–8151
https://doi.org/10.1007/s10570-019-02638-z

ORIGINAL RESEARCH

Enriched mechanical, UV shielding and flame retarding properties of cotton fabric coated with graphite nano platelets filled polyaniline–gum arabic nanocomposites

Preetam Bharadiya · Chetan Mahajan · Anil K. Sharma · Satyendra Mishra

Received: 7 February 2019 / Accepted: 18 July 2019 / Published online: 26 July 2019

Abstract Graphite nanoplatelets (GnP) were prepared by ultrasonication of thermally expanded graphite intercalated compound. In-situ oxidative polymerization was done to prepare GnP (1 wt%, 3 wt% and 5 wt%) filled polyaniline–gum arabic (GnP/PANI–GA) nanocomposites. These nanocomposites were further coated on the surface of the cotton fabric through the pad-dry-cure process. The characterization of the prepared nanocomposites and their coating was done by Fourier transform infrared spectroscopy and field emission scanning electron microscopy along with energy dispersive spectroscopy. Also, the mechanical, ultraviolet shielding and flame retarding properties of these coated fabrics were analysed as per ASTM D 5035, AATCC TM 183 and FMV SS 302 standards. 3 wt% GnP/PANI–GA nanocomposite coated fabric showed enriched tensile strength of (145 N) in weft direction, ultraviolet protection factor of 58, burn time of 173 s and limiting oxygen index of 26.10% as compared to 116 N, 5, 88 s and 18.3% respectively for the pure cotton fabric. Overall, the 3 wt% GnP/PANI–GA nanocomposite was evaluated as the optimum concentration because of the uniform dispersion of GnP in PANI/GA nanocomposite.

Keywords Graphite nanoplatelets · Polyaniline · Cotton · Gum arabic · UV shielding

Electronic supplementary material The online version of this article (https://doi.org/10.1007/s10570-019-02638-z) contains supplementary material, which is available to authorized users.

P. Bharadiya · S. Mishra (✉)
University Institute of Chemical Technology, Kavayitri Bahinabai Chaudhari North Maharashtra University, Jalgaon, Maharashtra 425001, India
e-mail: profsm@rediffmail.com

C. Mahajan · A. K. Sharma
Wool Research Association, P.O. Sandoz Baug, Kolshet Road, Thane, Maharashtra 400 607, India

Introduction

Graphene a monolayer of sp^2 hybridised carbon (Hansora et al. 2015) has attracted major research groups due to its excellent electronic, mechanical (Mahajan et al. 2018), electrical and thermal (Hu et al. 2015; Mishra and Hansora 2017) characteristics. However, the cost expensive and difficult synthesis make it essential to replace this graphene with similar other characteristic nanomaterial viz. graphite nanoplatelets (GnP), which consist of 10–30 layer graphene sheets (Nieto et al. 2012; Alam et al. 2015). GnP is a semi-metallic graphite crystal with thickness below 100 nm and other dimensions in several microns (Carotenuto et al. 2012). GnP find application in different areas such as supercapacitors, batteries, solar cells (Liu et al. 2010), biosensors (Aravind et al.

2011), corrosion resistance coatings (Šesta et al. 2018), fabric coatings (Hu et al. 2015), composites (Yasmin and Daniel 2004), actuators (Ozdemir et al. 2015) etc. because of ease of synthesis, higher surface area, excellent electrical, mechanical, ultraviolet (UV) shielding (Zhang et al. 2018a), flame retarding (Jeon et al. 2017) and EMI shielding properties (Bagotia et al. 2018) of GnP. GnP can cheaply be prepared from graphite intercalation compounds (GIC) by rapid thermal expansion and simultaneous ultrasonication in specific solvent (Alam et al. 2015).

Natural cellulose based cotton fabric finds application in different areas such as medicals, diapers, all types of clothing (Liu et al. 2018), medical electro-heating devices (Hao et al. 2018), dye sensitised solar cells (Sahito et al. 2015), filtration, nanocomposites (Nooralian et al. 2016) geo-polymer based composites (Alomayri et al. 2013, 2014), electronic transistors (Bourzac 2011), indoor decoration (Zhang et al. 2018b), sensors (Chen et al. 2016), etc. due to its extreme versatility in pure form or blended form, natural comfort, lower density, durability and biodegradability (Alomayri et al. 2014; Sahito et al. 2015). However, cotton fabric is hydrophilic in nature, easily absorbs dirt and moisture, and loses its strength after some cycles of water washing, shows poor resistance to ultraviolet rays (Gao et al. 2017) and also poor flame retardancy (Zhang et al. 2018b; Liu et al. 2018). These limitations make it less suitable for functional textiles based application.

Recently, one-dimensional polyaniline (PANI), due to ease of synthesis (Sen et al. 2018; Bharadiya et al. 2019), tunable conductivity, higher surface area, reverse doping-dedoping behaviour and good environmental stability (Tang et al. 2015; Sen et al. 2018; Bharadiya et al. 2019), finds application in various areas such as supercapacitors (Tang et al. 2015; Sen et al. 2018; Bharadiya et al. 2019; Jain et al. 2019), sensors (Sen et al. 2016, 2017, 2018), flame retarding materials (Mao et al. 2014; Yu et al. 2015), UV protective fabrics (Tang et al. 2015), anti-corrosive coating (Chang et al. 2012), etc. However, the poor compatibility and poor processability (Quintanilha et al. 2014) have declined its use for making nanocomposites with different nanomaterials required for coating of textiles. Therefore, in order to improve the processability and compatibility of PANI, natural polymer-gum arabic (GA) can be used as an emulsifier and green stabilizer (Quintanilha et al. 2014; Tiwari 2007) because of the presence of water loving carbohydrate groups and also hydrophobic protein groups (Quintanilha et al. 2014). GA consists of galactopyranose, arabinopyranose, arabinofuranose, ramnopyranose, glucuropyranosyluronic acid and 4-*o*-methylglucuropyronosyl uronic acid groups (Daoub et al. 2018) with small amount of calcium, magnesium and potassium salts (Singh et al. 2003; Montenegro et al. 2012). Due to its low cost, biodegradability, high molecular weight, amorphous nature (Tiwari 2007) and also higher reactivity with hydroxyl groups of water (Singh et al. 2003), GA suits as the best material to be used as a support for preparation of amorphous PANI (Tiwari 2007) and to get ease of compatibility with hydroxyl groups of cotton fabric in order to easily bind PANI on the cotton fabrics.

Different researches have been carried out on the coating of PANI, GnP or other nanomaterials on the various fabrics such as Graphene/PU coated cotton fabric (Hu et al. 2015), GnP coated PET fabrics (Zhang et al. 2018a), reduced graphene oxide coated cotton fabric for dye sensitised solar cells (Sahito et al. 2015), cotton fabric coated by geo polymer composites (Alomayri et al. 2013, 2014), flame retardant material coated cotton fabric (Zhang et al. 2018b), superhydrophobic TiO_2 coated cotton fabric (Gao et al. 2017), PANI/graphene oxide coated cotton fabric (Tang et al. 2015), PANI coated polyester fabric (Yu et al. 2015), waterborne anionic polyurethane-GnP coated cotton fabric (Qu et al. 2014), reduced graphene oxide coated cotton fabric for UV shielding (Pandiyarasan et al. 2017), enhanced electrical conductivity of polyester fabric based on silver colloid effect (Zhao et al. 2019), Graphene/MnO_2 based flexible fabric supercapacitors (Li et al. 2019), graphene coated 3D non-woven polyester pad based piezoresistive pressure sensors (Lu et al. 2019), Graphene/Tourmaline composite based cotton fabric joule heater (Hao et al. 2018), etc. But none of these showed the combined effect on the mechanical, UV shielding and flame retarding properties of the cotton fabric using GnP as a filler and GA as a stabilising and a supporting natural polymer with the conducting PANI. So far no reference was found using GnP filled polyaniline–gum arabic (GnP/PANI–GA) nanocomposites for preparation of functional textile. In the present work, considering the synergistic effect obtain with the combination of the conductive behaviour of PANI along with ease of compatibility and processability with GA and also the conductive,

thermal and mechanical properties with GnP; (1 wt%, 3 wt% and 5 wt% conc.) GnP/PANI–GA nanocomposites were prepared by in situ oxidative polymerization method and simultaneously coated on the cotton fabrics by facile pad-dry-cure process (Fig. 1) in order to enrich the mechanical, UV shielding and flame retarding properties of the cotton fabric. The chemical reactions occurring during the polymerization are shown in Fig. 2a, b.

Experimental

Raw materials

Graphite powder, Ammonium persulfate (APS), Aniline, Acetone and Gum arabic were purchased from S D fine chemicals, Mumbai, India. 98% Sulphuric acid (H_2SO_4), Nitric acid 69% (HNO_3), Methanol and Ethanol were purchased from Merck chemicals, Mumbai, India. All the chemicals were used without further purification. All the experiments were carried out with doubled distilled water.

Preparation of GnP, polyaniline–gum arabic (PANI–GA) nanocomposite and GnP filled polyaniline–gum arabic (GnP/PANI–GA) nanocomposites

For preparation of GnP, graphite powder (5 g), sulphuric acid (150 mL) and nitric acid (50 mL) were slowly added into a 500 mL flask and the mixture was stirred for 24 h at room temperature. The mixture was then poured slowly into 1 L water to collect the solid by filtration. The solid was washed using water for three times. After drying at 60 °C for 24 h, the GIC were obtained. The dry GIC powder was heated to 1000 °C for 10 s, cooled and simultaneously

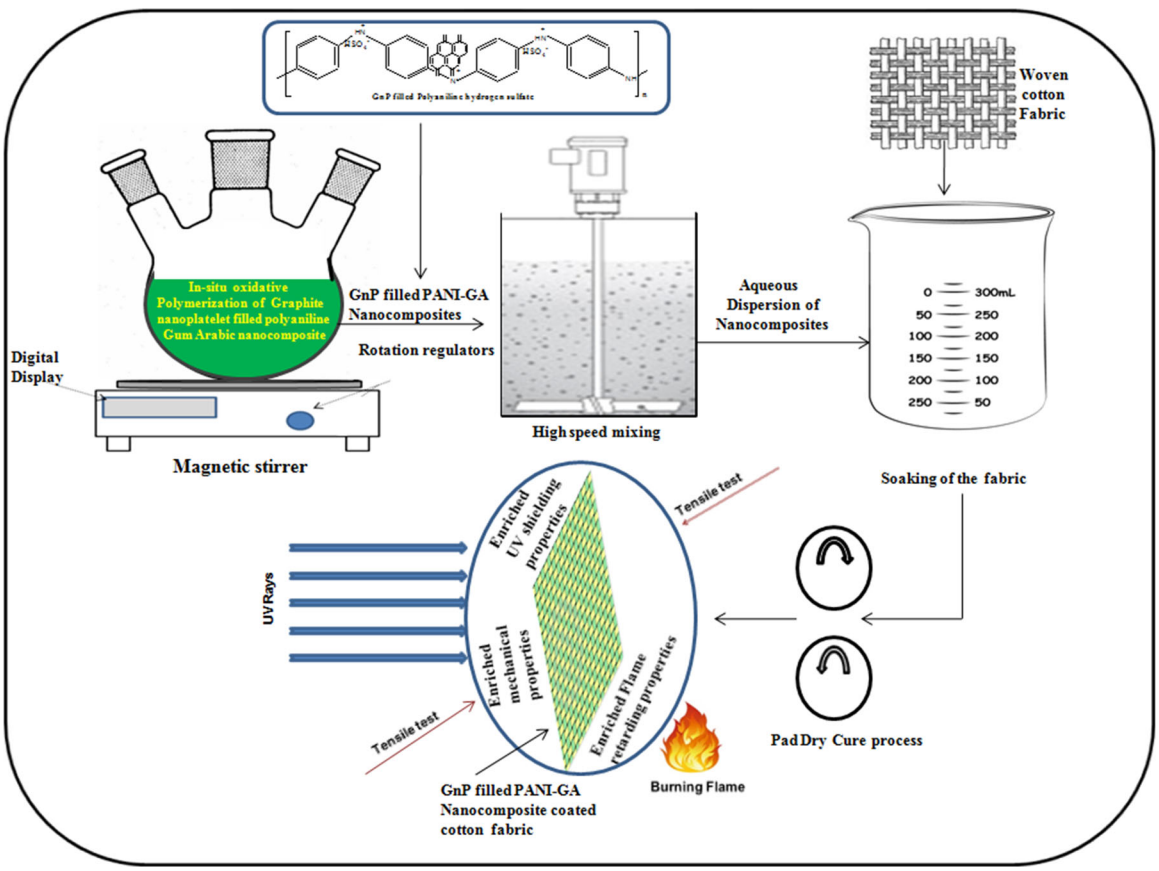

Fig. 1 Graphical abstract showing the GnP filled PANI–GA nanocomposites along with enrich mechanical, UV shielding and flame retarding properties

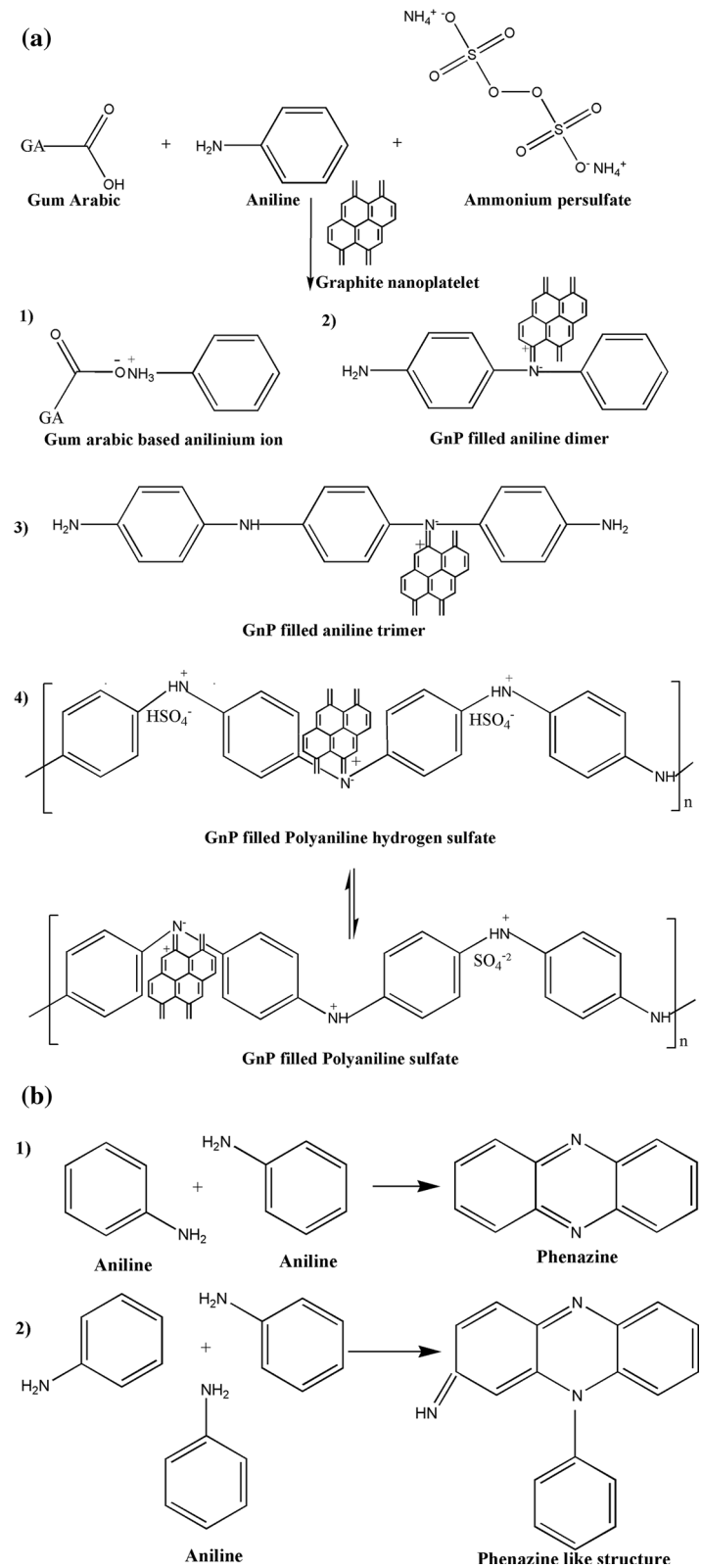

Fig. 2 **a** Chemical reactions involved in polymerization of GnP/PANI–GA nanocomposites. **b** Chemical reactions involved during phenazine formation

ultrasonicated in methanol for 4 h at room temperature; and finally filtered to give GnP powder.

For the preparation of PANI–GA nanocomposites, 1:1 weight ratio of gum arabic and Aniline were stepwise added along with 80 ml distilled water in the three neck flask followed by slow addition of 0.55 mol APS (dissolved in 40 ml distilled water). This solution was stirred for 24 h at room temperature, and then washed with water and acetone by centrifugation at 4000 rpm. The supernatant decanted away and solid residue was dried in oven at 60 °C for 24 h to get PANI–GA nanocomposites.

For the preparation of GnP/PANI–GA nanocomposites, GnP (1 wt%, 3 wt% and 5 wt% individual concentration of aniline), 1:1 weight ratio of gum arabic and Aniline were stepwise added along with 80 ml distilled water in the three neck flask. The remaining procedure was same as that for PANI–GA nanocomposites to obtain GnP/PANI–GA nanocomposites.

Coating of PANI–GA and GnP/PANI–GA nanocomposites on pure cotton fabric by pad dry cure method

The nanocomposites of different GnP concentrations were mixed separately in water with a liquor ratio of 1:30 using high speed mixer at 10,000 rpm for 30 min followed by ultrasonication for 3 h at room temperature. The woven pure cotton fabric of size (45 × 45) cm was allowed to soak this mixture for 15 min. This soaked fabric was dried by pad cure method at 50 °C. This process was repeated 2 times to get uniform coating on the entire cotton fabric.

Characterization of GnP, PANI–GA, GnP/PANI–GA nanocomposites, pure cotton fabric and cotton fabric coated by PANI–GA and GnP/PANI–GA nanocomposites

The Raman spectra of the GnP and GnP/PANI–GA nanocomposites were recorded on (Jobin–Yvon Horibra LABRAM HR-visible) Raman Spectrometer coupled with microscope in reflectance mode with 632.8 nm excitation laser source and a spectral resolution of 1 cm^{-1}.

The functional groups of the GnP, PANI–GA, GnP/PANI–GA nanocomposites, pure cotton fabric, cotton fabrics coated with PANI–GA and GnP/PANI–GA nanocomposites were judged by Fourier Transform Infrared Spectroscopy (FTIR Bruker, Germany) over the frequency range 500–4000 cm^{-1}. Each spectrum is average of 100 scans.

The morphologies of the GnP/PANI–GA nanocomposites were investigated by High Transmission Electron Microscopy (HRTEM, Model Tecnai G^2 F30, FEI America) while the morphologies of PANI–GA, GnP/PANI–GA nanocomposites, pure cotton fabric and cotton fabrics coated with PANI–GA and GnP/PANI–GA nanocomposites were investigated by Field Emission Scanning Electron Microscopy and Energy Dispersive X-ray Spectroscopy (FESEM, Model S-4800 Type II Hitachi High Technology Corporation Limited, Japan), operated at 15.0 keV.

The crystalline behaviour of the GnP, PANI–GA and GnP/PANI–GA nanocomposites was determined by (D8 Advance Bruker) Limited Germany, X-Ray Diffractometer (XRD) using monochromatic CuKα1 radiation (λ = 1.5406 Å) at 40 kV and 40 mA. The diffraction patterns were optimized with a step size of 0.020° over an angular range 5–80° (2θ) with a scanning speed of 1°/s.

Air permeability of the pure cotton fabric and the cotton fabrics coated with PANI–GA and GnP/PANI–GA nanocomposites were examined by air permeability equipment (SDL Atlas, Model MO2IA) using ISO 9237 standard. The crocking fastness to rubbing was measured by MAG Solvics Instrument, Coimbatore Tamil Nadu using ISO 105-X12. Both dry and wet tests were performed.

Thermal conductivity of the pure cotton fabric and the cotton fabrics coated with PANI–GA and GnP/PANI–GA nanocomposites were measured using Kawabata, Japan.

Mechanical property of the pure cotton fabric and the cotton fabrics coated with PANI–GA and GnP/PANI–GA nanocomposites were investigated by Instrument Testometric, UK using ASTM D 5035.The flexural rigidity and bending modulus were measured using Shirley Stiffness tester in warp direction as per IS 6490.

UV-shielding property of the pure cotton fabric and the cotton fabrics coated with PANI–GA and GnP/PANI–GA nanocomposites, as determined by UV protection factor (UPF) and UV transmission spectra were recorded by a UV spectrophotometer (UV1000F, Labsphere Inc., USA) using AATCC TM 183 standard.

Flame retarding property of the pure cotton fabric and the cotton fabrics coated with PANI–GA and GnP/PANI–GA nanocomposites were measured by (ATLAS, Hongkong) as per FMV SS 302 standard. The Limiting oxygen index test was measured by Oxygen Index apparatus (Shanta Eng, Thane India) as per ASTM D 2863. The test was carried out for 3 min.

Results and discussion

Structural and morphological properties of GnP filled PANI–GA nanocomposites

The structural defects of GnP, 1 wt%, 3 wt% and 5 wt% GnP/PANI–GA nanocomposites were confirmed by Raman Spectra (Fig. 3). For GnP, three characteristic peaks were observed at 1324 cm^{-1}, 1579 cm^{-1} and 2676 cm^{-1} corresponding to the structural defects (D peak), presence of sp^2 carbon network (G peak) and overtone of the D band i.e. 2D peak respectively (Nieto et al. 2012; Alam et al. 2015) (Fig. 3a). The I_D/I_G ratio was near to 0.58 and so there are fewer defects present in GnP; also the broad 2D peak confirms the occurrence of some multilayer graphene sheets in GnP (Nieto et al. 2012). For pure PANI–GA nanocomposite, the peaks were obtained at 611 cm^{-1}, 1165 cm^{-1}, 1337 cm^{-1}, 1589 cm^{-1} corresponding to the in plane benzene deformation, C–H bending of PANI, polaronic C–$N^{\cdot+}$ stretching and aromatic C–C stretching respectively (Fig. 3b). The

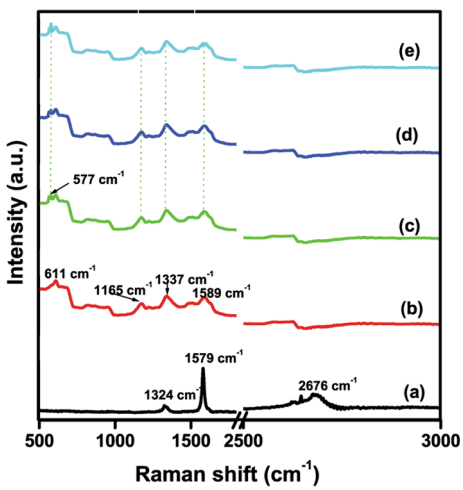

Fig. 3 Raman Spectra of (a) GnP, (b) PANI–GA, (c) 1 wt%, (d) 3 wt% and (e) 5 wt% GnP/PANI–GA nanocomposites

last two bands confirmed the conducting state of PANI. With addition of 1 wt%, 3 wt% and 5 wt% GnP, a new peak at 577 cm^{-1} was obtained corresponding to the crosslinked structure of PANI because of formation of phenazine structure (Quintanilha et al. 2014; da Silva et al. 2005) (Fig. 3c–e). This phenazine structure was responsible for formation of nanotubes of PANI. No separate GnP peak was observed in 1 wt% and 3 wt% GnP/PANI–GA nanocomposites. This may be due to proper interaction of GnP with PANI–GA nanocomposites. But for 5 wt% GnP/PANI–GA nanocomposite, the aromatic C–C stretching peak was overlapped with the G peak of GnP. This is because of improper interaction of all GnP with PANI–GA nanocomposite. Also, the decrease in intensity of aromatic C–C stretching and polaronic C–$N^{\cdot+}$ stretching peaks was noticed in 5 wt% GnP/PANI–GA nanocomposites due to poor oxidation of PANI. Thus, raman spectroscopy confirms the formation of GnP/PANI–GA nanocomposites.

Also, the functional groups of GnP/PANI–GA nanocomposites were investigated using FTIR (Fig. 4). For GnP, the peak was observed at 2115 cm^{-1} corresponding to the weak C=C bond (Fig. 4a). For pure PANI–GA nanocomposites, the peak at 3235 cm^{-1} was assigned to strong interaction of OH group in GA with amine group of PANI, due to hydrogen bond (Quintanilha et al. 2014). Other peaks observed at 1569 cm^{-1} were due to C=C of quinoid (Q) group, at 1491 cm^{-1} indicating benzenoid stretching, at 1443 cm^{-1} for N=N stretching, at 1414 cm^{-1} due to formation of phenazine structure, at 1289 cm^{-1} due to C–N bond, at 1147 cm^{-1} indicating N=Q=N stretching, at 1040 cm^{-1} because of SO_3^- group on aromatic ring, at 821 cm^{-1} for C–H out of plane deformation of (1,4 disubstituted ring), 696 cm^{-1} for (C–H) out of plane ring bending of monosubstituted ring and 589 cm^{-1} for HSO_4^- respectively (Fig. 4b) (Trchová and Stejskal 2011). As compared to pure PANI–GA nanocomposite, from (Fig. 4c, d) for 1 wt% GnP and 3 wt% GnP/PANI–GA nanocomposites the peaks are slightly red shifted or blue shifted and no new peaks were observed as shown in Table S1. This shift is due to good interaction of GnP with PANI after reduction of its interfacial tension in PANI–GA nanocomposites by GA. But for 5 wt% GnP/PANI–GA nanocomposite, the decrease in the intensity of C–N bond stretching and N=Q=N bond stretching reveals poor protonation of this nanocomposites (Fig. 4e).

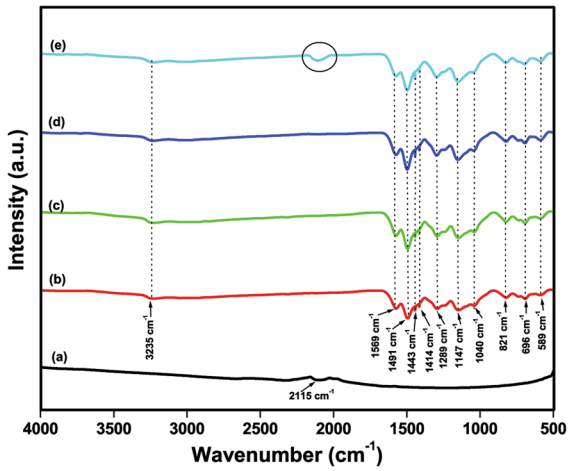

Fig. 4 FTIR of (a) GnP, (b) PANI–GA, (c) 1 wt%, (d) 3 wt% and (e) 5 wt% GnP/PANI–GA nanocomposites

This is further confirmed from the decrease in the degree of oxidation for 5 wt% GnP/PANI–GA nanocomposite (Table S1). The reason for this is poor protonation of PANI is due to less availability of carboxyl group of GA for oxidization of aniline. This is because with higher concentration of GnP (5 wt%) mostly all GA are required to reduce the interfacial tension and to stabilise the GnP in PANI. Also, the occurrence of the C=C bond of GnP at 2115 cm^{-1} for 5 wt% GnP/PANI–GA nanocomposite reveals that the amount of GA used was insufficient for interaction and stabilisation of all GnP in PANI. Thus, FTIR analysis showed the formation of nanocomposites of PANI with GA using GnP as a filler. It also showed that GnP and PANI are well interacted and dispersed with the presence of GA in PANI, up to 3 wt% GnP concentration.

The morphological properties of GnP/PANI–GA nanocomposites were confirmed by HRTEM analysis as shown in Fig. 5. A typical HRTEM image of GnP is shown in (Fig. 5a), in which few number of overlapped graphite nano platelets can be observed having thickness below 10 nm and lateral size < 200 nm. For pure PANI–GA nanocomposites, the non-uniform and random morphology was obtained (Fig. 5b). With addition of 1 wt% GnP in PANI–GA, the formation of nanotubes begins due to formation of phenazine structure (Fig. 5c). The increase in concentration of GnP results in more formation of PANI–GA nanotubes in the structure as well as the circular and non-uniform structures (Fig. 5d, e). Thus, it is confirmed that GnP favors the formation of nanotubular structures.

The morphology and elemental mapping of the PANI–GA nanocomposites were further detected by FESEM–EDS (Fig. 6). For pure PANI–GA nanocomposite, the non-uniform micelles and random flakes like morphology was observed (Fig. 6a). After addition of 1 wt% GnP in the PANI–GA nanocomposite, the formation of nanotubes begins in the nanocomposite (Fig. 6b). With increase in GnP concentration from 3 to 5 wt% in the PANI–GA nanocomposites, the nanotubes morphology starts dominating the non-uniform micelles and flake like morphology (Fig. 6c, d). This might be occurring because of following reasons. For PANI–GA nanocomposite; when aniline is added to the GA solution and APS is added simultaneously than two types of acidic groups are available, (1) as the carboxyl group of GA and (2) as the sulphuric acid obtained by the decomposition of APS. Therefore, the acidity of the reaction increases with time due to the generation of more protons of carboxyl and sulphuric acids groups, which favours the random non-uniform morphology (Trchova et al. 2006). For 5 wt% GnP/PANI–GA nanocomposite all GA is consumed for the interaction and stabilisation of GnP and this led to the availability of only sulphuric acid groups as a acidic medium for aniline. Thus, the acidity of the reaction with time is not much increased and the sulphuric acid favours the formation of phenazine structure in the PANI which finally favours the nanotube morphology (Trchova et al. 2006). This is also confirmed from the decrease in the oxidation of the PANI–GA nanocomposite for 5 wt% GnP concentration as shown in Table S1.

The EDS shows that PANI–GA nanocomposite contains elements such as Carbon, Oxygen, Nitrogen, Sulphur, Potassium, Magnesium and Calcium (Fig. S1a). But with increase in GnP concentration (5 wt%), the Carbon content increases due to increase in the graphitic carbon concentration (Fig. S1b).

The crystalline behaviours of pure PANI–GA and all GnP/PANI–GA nanocomposites were confirmed by XRD analysis (Fig. 7). The XRD peaks of GnP were observed at 25.63° (002), 41.62° (100), 43.66° (101), 53.76° (004) and 76.71° (110) respectively

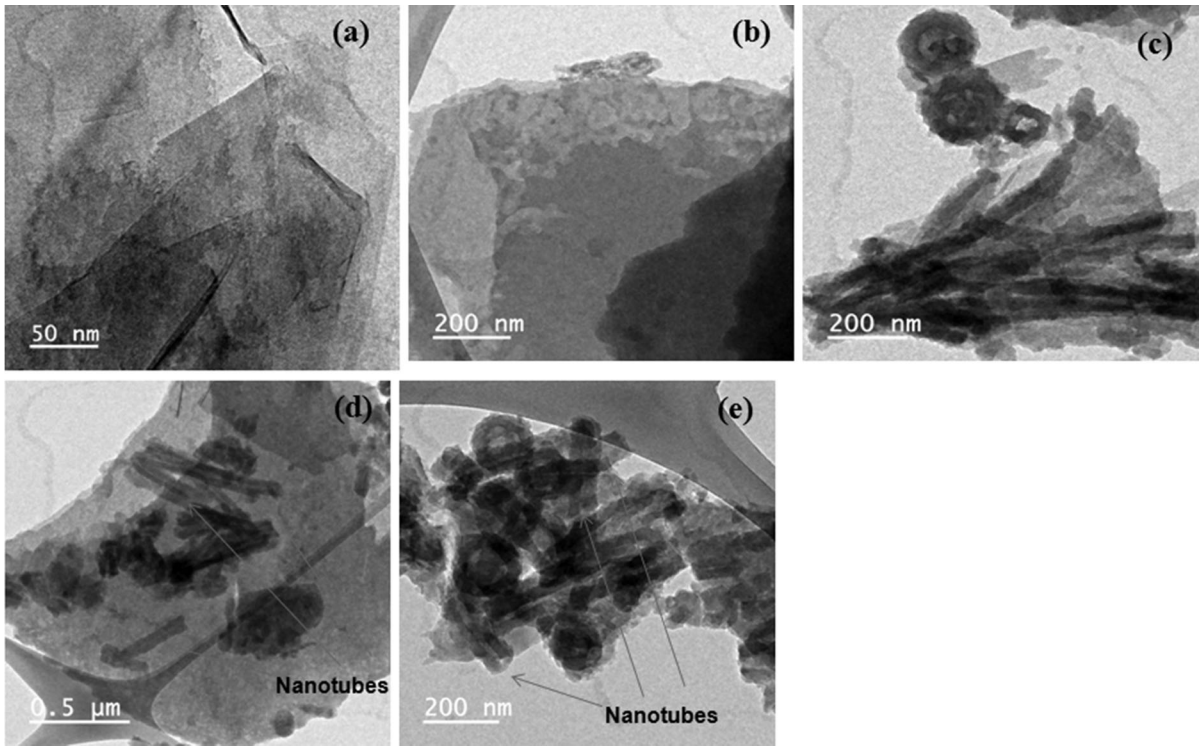

Fig. 5 HRTEM images of **a** GnP, **b** PANI–GA, **c** 1 wt% PANI–GA, **d** 3 wt% PANI–GA, **e** 5 wt% PANI–GA nanocomposites

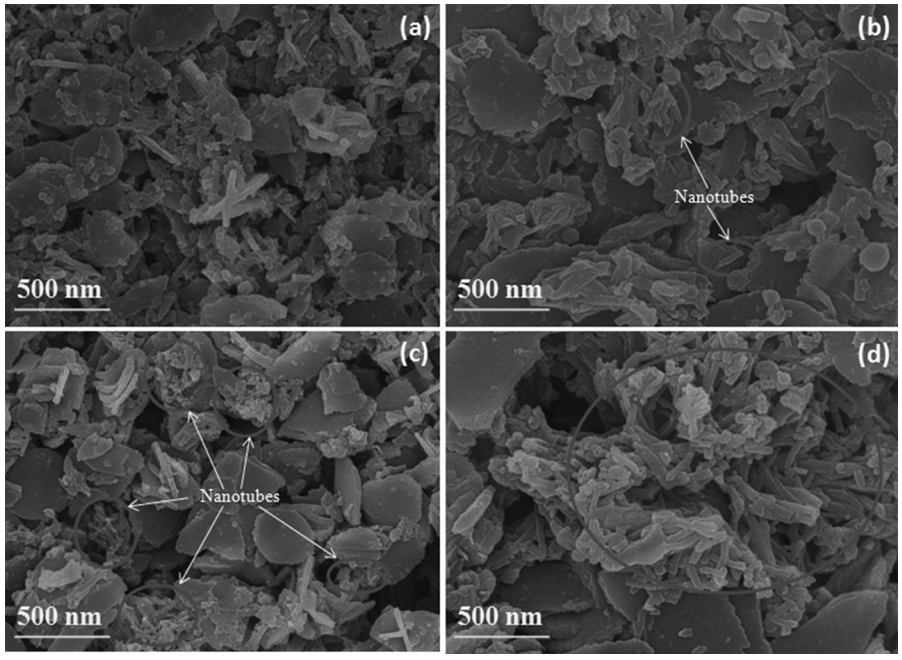

Fig. 6 FESEM of **a** PANI–GA, **b** 1 wt%, **c** 3 wt% and **d** 5 wt% GnP/PANI–GA nanocomposites

(Alam et al. 2015), confirming the highly crystalline nature of the prepared GnP (Fig. 7a). For PANI–GA nanocomposite, the broad peaks were obtained at 18.59°, 19.64°, 23.54° and 25.79° confirming the partially crystalline nature of the PANI–GA nanocomposites (Fig. 7b). These broad peaks can be assigned to the periodicity parallel and perpendicular to the polymer chains of PANI (Zhang et al. 2007). But with GnP the number of peaks were increased due to proper stabilisation of GnP with PANI using GA as a stabilising agent thereby, increasing the crystalline behaviour. For 5 wt% GnP/PANI–GA nanocomposite, the peaks were obtained at 6.34°, 18.59°, 19.64°, 23.33°, 25.82°, 26.48°, 39.77°, 42.41°, 44.36° and 54.41° (Fig. 7c). The peak obtained at lower degree (6.34°) angle was due to the incorporation of nano-sized platelets of graphite in PANI while the occurrence of weak peak at 25.82° confirmed the presence of few amount of non-interacted GnP and the different peaks at 26.48°, 39.77°, 42.41°, 44.36°, 54.41° revealed that major amount of GnP was properly interacted and stabilised with PANI using GA as a dispering agent in the 5 wt% GnP/PANI–GA nanocomposite. Thus, the amount of GA used was sufficient to incorporate crystallinity by well interaction of major amount of GnP with PANI thereby decreasing the amorphous behaviour of the pure PANI–GA nanocomposite. But minor amount of GnP was not properly interacted within the 5 wt% GnP/PANI–GA nanocomposite.

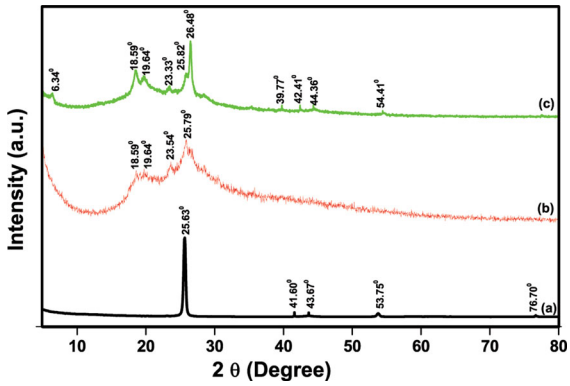

Fig. 7 XRD of (a) GnP, (b) PANI–GA and (c) 5 wt% GnP/PANI–GA nanocomposites

Morphology and structure of GnP/PANI–GA nanocomposites coated cotton fabric

The surface morphology of the GnP/PANI–GA nanocomposites coated cotton fabrics were shown in Fig. 8. For pure cotton fabric, pure flat surface of the interlaced cotton fabric was noticed (Fig. 8a). With pure PANI–GA nanocomposite coated fabric, the overall surface was observed to be bumpy in nature due to the deposition of PANI–GA nanocomposites (Fig. 8b). But with 5 wt% GnP/PANI–GA nanocomposite, bumby surface was observed along with good bonding of the GA dispersed GnP/PANI with the cotton fiber (Fig. 8c).

The elements present in the pure cotton fabric are Carbon and Oxygen (Fig. S2a). For PANI–GA nanocomposite (Fig. S2b) and 5 wt% GnP/PANI–GA nanocomposite coated cotton fabric (Fig. S2c), the elements present are Carbon, Oxygen, Nitrogen, Sulphur, Potassium, Calcium and Magnesium. Only thing is that the carbon content increases with GnP concentration in the 5 wt% GnP/PANI–GA nanocomposites confirming the good deposition of GnP/PANI–GA nanocomposites on the cotton fabric respectively.

The FTIR peaks of the pure cotton fabric and PANI–GA nanocomposites coated cotton fabrics are shown in Fig. 9. For pure cotton fabric the important peaks were observed at 3275 cm^{-1} for OH group, 2893 cm^{-1} for CH_2 existence, 1738 and 1627 cm^{-1} for C=O stretching, 1426 cm^{-1} for C–C symmetric stretching, 1365 cm^{-1} and 1312 cm^{-1} for CH bending, 1155 cm^{-1} and 1019 cm^{-1} for C–O bending of cellulose, 894 cm^{-1} for C–C stretching, 662 cm^{-1} for C–OH out of plane bending respectively (Fig. 9a). With PANI–GA nanocomposite coated cotton fabric, the additional peaks at 1491 cm^{-1}, 1444 cm^{-1}, 1415 cm^{-1}, 1298 cm^{-1}, 821 cm^{-1}, 696 cm^{-1} and 589 cm^{-1} were observed which are the characteristic peaks of the pure PANI–GA nanocomposites (Fig. 9b). Also, for all GnP/PANI–GA nanocomposites (Fig. 9c–e), these peaks are slightly red shifted or blue shifted and no new peak is observed due to interaction of GnP with PANI–GA nanocomposites coated on cotton fabric. In case of the 5 wt% GnP/PANI–GA nanocomposite coated cotton fabric, the decrease in intensity of the C–N bond stretching and N=Q=N bond stretching reveals poor doping of this nanocomposite due to less oxidation. But the

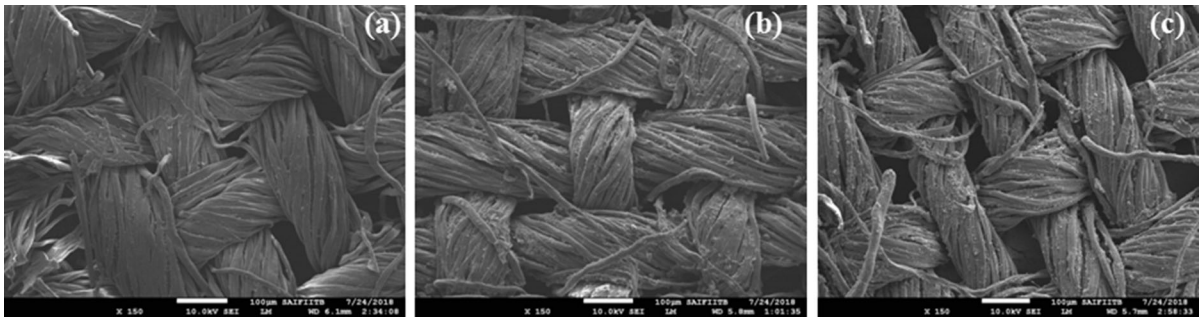

Fig. 8 FESEM-EDS of **a** pure cotton fabric and cotton fabric coated with **b** PANI–GA and **c** 5 wt% GnP/PANI–GA nanocomposites

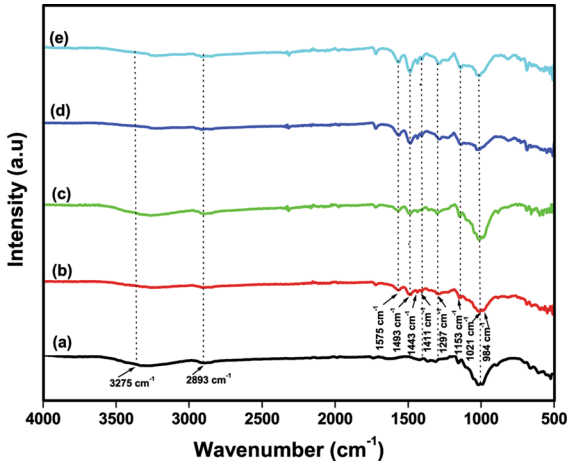

Fig. 9 FTIR of (a) pure cotton fabric and cotton fabric coated with (b) PANI–GA, (c) 1 wt%, (d) 3 wt% and (d) 5 wt% GnP/PANI–GA nanocomposites

deposition of PANI–GA and all GnP/PANI–GA nanocomposites were properly obtained on the cotton fabric.

Air permeability and crocking fastness of GnP/PANI–GA nanocomposites coated cotton fabric

Air permeability values of GnP/PANI–GA nanocomposites coated cotton fabrics are listed in Table 1. Compared to the pure cotton fabric, the air permeability K decreases in larger extent for cotton fabric coated with PANI–GA, 1 wt% and 3 wt% GnP/PANI–GA nanocomposites. This larger decrement in air permeability is because of two reasons (1) uniform coating of the GnP/PANI–GA nanocomposites on the cotton fabric. (2) GA functional groups support proper chemical bonding of GnP/PANI nanocomposites with the cellulose groups of the cotton fabric and also penetrate into the amorphous region of the pure cotton fabric, thereby obstructing the air flow. GnP is impermeable to gases (Kim et al. 2010) and so the air permeability decreases with increase in GnP concentration due to increase in graphitic network on the surface of the cotton fabric. But for 5 wt% GnP/PANI–GA nanocomposite, the air permeability increases due to poor protonated form of PANI, non-uniform distribution and poor stability of all GnP in PANI with GA, reducing the obstruction of air flow.

The crocking fastness of pure cotton fabric, cotton fabric coated with PANI–GA and all GnP/PANI–GA nanocomposites are shown in Table 1. For pure cotton fabric, it was highest in both dry and wet tests. With PANI–GA coated fabric, it decreases to 3–4 for dry test, and 2 for wet test. This decrease is because of removal of amorphous PANI–GA from the surface of cotton fabric after rubbing. With 1 wt%, 3 wt% and 5 wt% GnP/PANI–GA nanocomposites coated fabric, it again reduces to 3 for dry test, and 1–2 for wet test. This decrease in crocking fastness for all nanocomposites as compared to pure PANI–GA nanocomposite coated fabric is due to removal of some amount of GnP along with PANI–GA from the surface of cotton fabric. The decrease in value for wet test in all the nanocomposites coated cotton fabric is due to removal of hydrophilic GA groups from the surface responsible for bonding of the GnP/PANI nanocomposites.

Electrical and thermal conductivity characteristics of GnP/PANI–GA nanocomposites coated cotton fabric

The electrical conductivity of the GnP/PANI–GA nanocomposites coated fabrics were calculated from I–V curves according to Ohm's law (Table 2). Cotton

Table 1 Air permeability and crocking fastness of cotton fabric coated with PANI–GA and GnP/PANI–GA nanocomposites

Sr. no.	Name of the coated fabric	Air permeability (dm^3/s)	Crocking fastness	
			Dry test	Wet test
1	Pure cotton fabric	3.12	5	5
2	PANI–GA	0.83	3–4	2
3	1 wt% GnP/PANI–GA	0.64	3	1–2
4	3 wt% GnP/PANI–GA	0.53	3	1–2
5	5 wt% GnP/PANI–GA	0.70	3	1–2

fabric is non-conducting in nature but with PANI–GA coating, some amount of conductivity was introduced. An increment in electrical conductivity was noticed for 1 wt% and 3 wt% GnP/PANI–GA nanocomposites coated cotton fabrics due to conductive nature of the GnP. But this much conductivity is not sufficient to give electromagnetic interference shielding. The low extent of conductivity obtained here was because of the absence of acidic medium during the synthesis of PANI which resulted in formation of nanotubular structure and non-uniform structure (Sapurina and Stejskal 2008). As compared to 1 wt% and 3 wt% GnP/PANI–GA nanocomposites coated fabric, 5 wt% GnP/PANI–GA nanocomposite coated fabric showed decrement in conductivity due to interruption of network for electrons within the polymer matrix as the concentration of GnP was greater than 2 wt% (Li et al. 2005).

Thermal conductivity values of GnP/PANI–GA nanocomposites coated cotton fabrics are illustrated in Table 2. The thermal conductivity for the fabrics were obtained by following equation:

$$K = \frac{W \times D}{A \times \Delta T} (W/cm\ ^{\circ}C)$$

where D is the thickness (cm), A is the area of heating plate (cm), ΔT is the (temperature of BT box)-(temperature of constant base), W is the heat flow of BT Box (heat loss).

For pure cotton fabric, the conductivity obtained is 2.48×10^{-5} W/m K. But PANI–GA nanocomposite coated fabric shows the highest increment due to availability of overall amorphous phase throughout the area for the passage of heat. However, for 1 wt% GnP/PANI–GA nanocomposite coated fabric, it again decreases due to incorporation of crystalline phase in the nanocomposite with addition of GnP. It decreases further for 3 wt% GnP/PANI–GA nanocomposite due to uniform distribution of GnP in the PANI which leads to an increase in time for passage of heat from amorphous to crystalline phase and vice versa. But for 5 wt% GnP–PANI–GA nanocomposite, it further increases due to increase in concentration of crystalline GnP and also due to presence of some non-interacted GnP.

Mechanical properties of GnP/PANI–GA nanocomposites coated cotton fabric

Mechanical properties of GnP/PANI–GA nanocomposites coated cotton fabric are shown in Fig. 10a, b. As compared to pure cotton fabric the tensile strength and % elongation are slightly increased for PANI–GA nanocomposite coated fabric in warp direction, but decreases for 1 wt% GnP/PANI–GA nanocomposite coated fabric, followed by further increase for 3 wt% and 5 wt% GnP/PANI–GA nanocomposites coated fabric in warp direction. In case of weft direction, the

Table 2 Electrical and thermal conductivity of cotton fabric coated with PANI–GA and GnP/PANI–GA nanocomposites

Sr. no.	Name of the sample	Electrical conductivity (S/cm)	Thermal conductivity (W/m K) $\times 10^{-5}$
1	Pure cotton fabric	0	2.48
2	PANI–GA	3.35×10^{-8}	3.07
3	1 wt% GnP/PANI–GA	1.02×10^{-8}	2.93
4	3 wt% GnP/PANI–GA	2.79×10^{-7}	2.56
5	5 wt% GnP/PANI–GA	1.44×10^{-7}	2.83

tensile strength shows increasing trend up to 3 wt% GnP/PANI–GA nanocomposites coated fabric due to the uniformly distributed GnP in PANI with GA. But for 5 wt% GnP/PANI–GA nanocomposite, it decreases due to the unstability of all GnP in PANI with GA. The % elongation shows different trend for the nanocomposites coated fabric in the order as PANI–GA < 3 wt% GnP/PANI–GA < 1 wt% GnP/PANI–GA < cotton < 5 wt% GnP/PANI–GA nanocomposites (Fig. 10b). Thus, it is confirmed that 5 wt% GnP/PANI–GA nanocomposite coated fabric shows enriched mechanical properties in warp direction while 3 wt% GnP/PANI–GA nanocomposite coated fabric shows that in weft direction respectively.

The flexural rigidity and bending modulus of the GnP/PANI–GA nanocomposites coated cotton fabric are shown in Table 3.

The flexural rigidity was calculated by the formula below (Saville 2002)

$$G = W \times \left(C^3\right) \times 9.807 \times 10^{-6}\ \mu Nm$$

where W is the weight per unit area of the fabric in grams per square meters. C is the bending length in mm.

The flexural rigidity of pure cotton fabric was obtained as 9.29 μNm. For pure PANI–GA, 1 wt%, 3 wt% and 5 wt% GnP/PANIGA nanocomposites coated fabrics, the flexural rigidity were observed as 7.57, 9.04, 9.60 and 8.47 μNm. The flexural rigidity decreased for PANI–GA nanocomposites coated fabric because of depolymerization of cellulose group of cotton fabric by carboxyl group of GA. The rigidity was found to increase for 1 wt% and 3 wt% GnP/PANI–GA nanocomposite coated cotton fabric because the incorporation of GnP increases the stiffness of the fabric. But for 5 wt% GnP/PANI–GA nanocomposite coated fabric, the flexural rigidity was further decreased due to non-uniform distribution of the GnP on the cotton fabric making the fabric less stiffer than the previous ones.

The bending modulus was calculated from the formula given below (Saville 2002)

$$\text{Bending modulus} = \frac{12 \times G \times 10^3}{T^3}\ N/m^2$$

where, T = fabric thickness in mm and 1 N/m^2 = 0.0001 N/cm^2.

Like flexural rigidity, the bending modulus showed similar behavior (Table 3). For cotton fabric, it was 32.50 N/cm^2. It decreased for PANI–GA coated fabric to 26.6 N/cm^2 because of reaction of carboxyl group of GA with cellulose group of cotton fabric. As compared to PANI–GA nanocomposite coated cotton fabric, for 1 wt% and 3 wt% GnP/PANI–GA nanocomposites coated cotton fabric, it further increased to 29.0 and 30.8 N/cm^2 due to increasing GnP concentration which increases the stiffness. But for 5 wt% GnP coated fabric, it further decreased to 27.2 N/cm^2 due to non-uniform distribution of GnP over the surface of the cotton fabric. All the values of

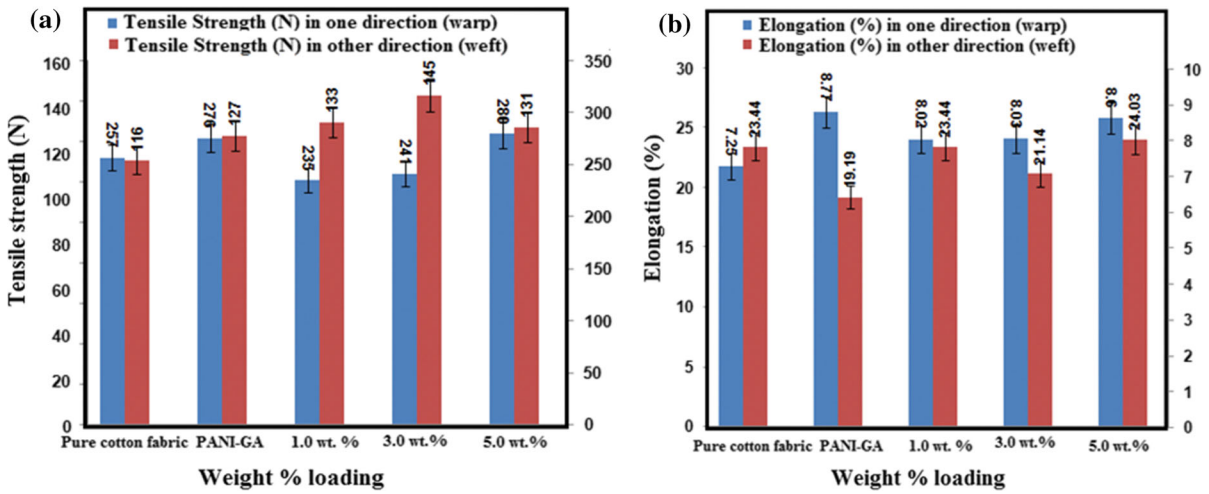

Fig. 10 **a** Tensile strength and **b** elongation (%) in one direction (warp) and other direction (weft) for pure cotton fabric and cotton fabric coated with PANI–GA, 1 wt%, 3 wt% and 5 wt% GnP/PANI–GA nanocomposites

Table 3 Flexural rigidity and bending modulus of cotton fabric coated PANI–GA and GnP/PANI–GA nanocomposites

Sr. no.	Name of the sample	Flexural rigidity (μNm)	Bending modulus (N/cm^2)
1	Pure cotton fabric	9.29	32.5
2	PANI–GA	7.57	26.6
3	1 wt% GnP/PANI–GA	9.04	29.0
4	3 wt% GnP/PANI–GA	9.60	30.8
5	5 wt% GnP/PANI–GA	8.47	27.2

bending modulus of coated fabric were lower than pure cotton fabric because the reaction of carboxyl group of GA with cellulose of cotton fabric resulted in depolymerization of the cellulose group of the fabric (Yang et al. 2000).

UV Shielding properties of GnP/PANI–GA nanocomposites coated cotton fabric

UV shielding properties of GnP/PANI–GA nanocomposites coated cotton fabric are shown in Fig. 11a, b. PANI–GA nanocomposite coated fabric shows the UV shielding behaviour because of the presence of GA which crosslinks its structure (Kuan et al. 2009). As compared to pure cotton fabric and PANI–GA nanocomposites coated fabric, the UV shielding and ultraviolet protection factor (UPF) shows increasing trend for 1 wt% and 3 wt% GnP/PANI–GA nanocomposite coated fabrics respectively. The mechanism for the enriched UPF can be explained as above. GnP present in the nanocomposites absorb maximum UV light and dissipate it in the form of heat without any chemical reaction. GA present in the nanocomposite crosslinks its structure and thus, supports GnP for shielding the fabrics from the harmful UV rays. Also, the increasing absorption of UV rays with increasing concentration and the uniform distribution of GnP throughout the fabrics makes the 3 wt% GnP/PANI–GA nanocomposite coated fabric to show the highest UV shielding behaviour. But with 5 wt% GnP/PANI–GA nanocomposite coated fabric, it further decreases due to saturation of the pure cotton fabric and poor stability of all GnP in PANI–GA. Thus, 3 wt% GnP/PANI–GA nanocomposite coated cotton fabric shows the overall enriched results.

Flame retarding property of GnP/PANI–GA nanocomposite coated cotton fabrics

Flame retarding property of GnP/PANI–GA nanocomposites coated cotton fabrics are shown in Fig. 12 and Figure S3. The flame retardancy was tested in terms of burn time (second). As compared to pure cotton fabric, the burn time shows increasing trend with increasing concentration of GnP in the PANI–GA nanocomposite. With increase in temperature, GnP endothermically reacts with the oxygenated groups in the cotton fabrics and PANI–GA nanocomposites. Thus, it maintains the surface temperature of the coated fabrics to a lower degree. Also, the graphitic network on the surface of cotton fabrics blocked the contact between coated fabric and oxygen directly thereby, increasing the flame retardancy of the cotton fabric with increase in GnP concentration. Thus, 5 wt% GnP/PANI–GA nanocomposite shows the highest value of burn time as compared to other nanocomposites.

The LOI graph of pure cotton fabric and cotton fabric coated with PANI–GA and GnP/PANI–GA nanocomposites are shown in Fig. 12. LOI values of 18.3, 21.2, 23.6, 26.1 and 27.3% were obtained for pure cotton fabric and cotton fabric coated with PANI–GA, 1 wt%, 3 wt% and 5 wt% GnP/PANI–GA nanocomposites respectively. The LOI increases with the coating of the PANI–GA because of higher energy required for burning of the polymer molecules. With addition of GnP, LOI further increases up to 3 wt% due to good flame retarding behaviour of GnP and also proper bonding of PANI–GA with GnP coated on the fabric. But with 5 wt% GnP concentration, LOI decreases because of poorly distributed GnP on the entire surface of the cotton fabric. Thus, LOI also supports the flame retarding behaviour of cotton fabric coated with GnP/PANI–GA nanocomposites.

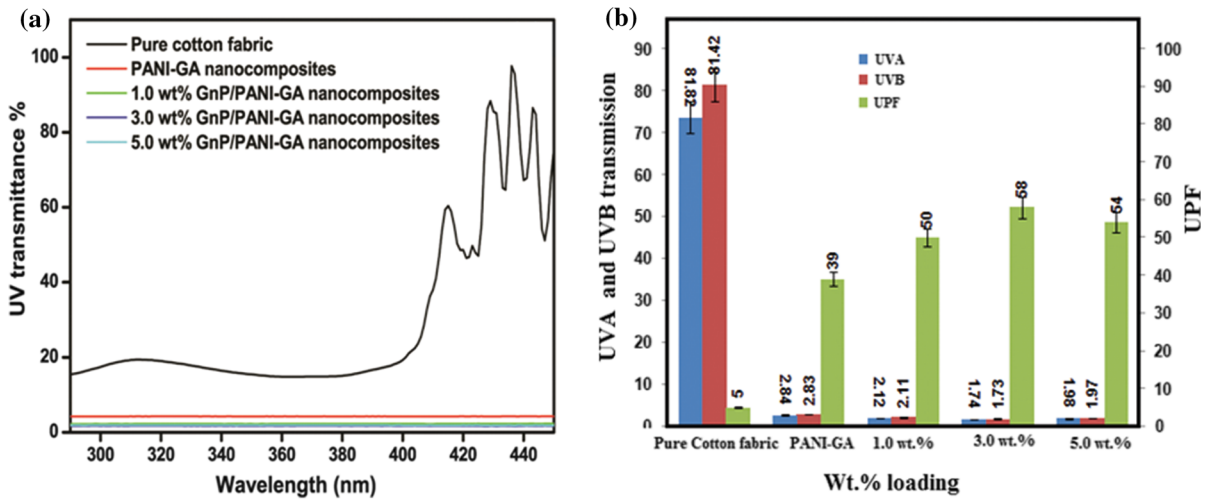

Fig. 11 **a** UV transmission spectrum and **b** UVA, UVB and UPF transmittance values for pure cotton fabric and cotton fabric coated with PANI–GA, 1 wt%, 3 wt% and 5 wt% GnP/PANI–GA nanocomposites

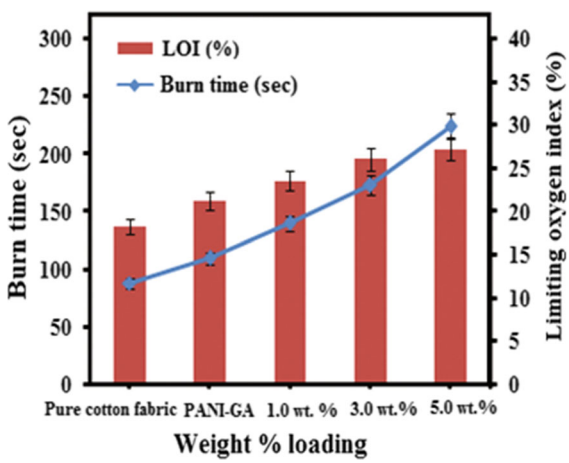

Fig. 12 Flame retarding property for pure cotton fabric and cotton fabric coated with PANI–GA, 1 wt%, 3 wt% and 5 wt% GnP/PANI–GA nanocomposites

Conclusions

GnP was prepared by thermal exfoliation method. HRTEM, XRD, FTIR and Raman confirm the formation of multilayer graphene sheets with good crystallinity. Different wt% GnP/PANI–GA nanocomposites were prepared by in situ oxidation polymerization and coated on the pure cotton fabric. HRTEM and FESEM images of the PANI–GA nanocomposites showed the formation of non-uniform structure. But with GnP filler, the nanotubes morphology was more dominant in the structure of the nanocomposites. Raman and FTIR spectra confirmed the formation of PANI–GA nanocomposite and also revealed good interaction of PANI with GnP in presence of GA as a stabiliser up to 3 wt% GnP concentration. XRD of PANI–GA nanocomposite revealed its amorphous nature but further addition of GnP produces crystallinity in it. FTIR of pure cotton fabric coated with PANI–GA and GnP/PANI–GA nanocomposite revealed the fixation of polymer groups on the cotton fabric. As compared to pure cotton fabric, for 3 wt% GnP/PANI–GA nanocomposite coated fabric, air permeability showed a decrease in 16% value, tensile strength in weft direction and thermal conductivity showed an increase in 1% value, UPF showed increase in 11.7% value, flame retarding property showed increase in 2.5% and LOI showed increase of 1.5% respectively. Overall 3 wt% GnP/PANI–GA nanocomposite coated cotton fabric showed good enrichment in mechanical, ultraviolet shielding and flame retarding properties of the fabric as compared to other nanocomposites coated fabric due to proper incorporation of GnP in the PANI using GA as stabiliser and supporting agent. Also, 5 wt% GnP/PANI–GA nanocomposite was not properly stabilised due to non-availability of all GA groups which leads to poor oxidation and the fabric was saturated above 3 wt% GnP/PANI–GA coating. This leads to its poor properties as compared to 3. wt% GnP/PANI–GA nanocomposite. Thus, 3 wt% GnP coated fabric can be utilised for military based application requiring higher mechanical, UV shielding and flame retarding properties.

Acknowledgments PSB is thankful to TEQIP-III, MHRD, New Delhi for financial assistance.SM is thankful to UGC, New Delhi for granting BSR Faculty Fellowship.

References

Alam SN, Kumar L, Sharma N (2015) Development of Cu-exfoliated graphite nanoplatelets (xGnP) metal matrix composite by powder metallurgy route. Graphene 4:91–111. https://doi.org/10.4236/graphene.2015.44010

Alomayri T, Shaikh FUA, Low IM (2013) Thermal and mechanical properties of cotton fabric-reinforced geopolymer composites. J Mater Sci 48:6746–6752. https://doi.org/10.1007/s10853-013-7479-2

Alomayri T, Shaikh FUA, Low IM (2014) Synthesis and mechanical properties of cotton fabric reinforced geopolymer composites. Compos Part B 60:36–42. https://doi.org/10.1016/j.compositesb.2013.12.036

Aravind SSJ, Baby TT, Arockiadoss T, Rakhi RB, Ramaprabhu S (2011) A cholesterol biosensor based on gold nanoparticles decorated functionalized graphene nanoplatelets. Thin Solid Films 519:5667–5672. https://doi.org/10.1016/j.tsf.2011.03.032

Bagotia N, Mohite H, Tanaliya N, Sharma DK (2018) A comparative study of electrical, EMI shielding and thermal properties of graphene and multiwalled carbon nanotube filled polystyrene nanocomposites. Carbon Nanotube Compos 39:E1041–E1051. https://doi.org/10.1002/pc.24465

Bharadiya PS, Jain R, Chaudhari V, Mishra S (2019) Graphene oxide wrapped polyaniline nanorods for supercapacitor application. Polym Compos. https://doi.org/10.1002/pc.25129

Bourzac K (2011) Cotton transistors weave comfort into electronics. New Sci 212(2837):22–23. https://doi.org/10.1016/S0262-4079(11)62712-7

Carotenuto G, De Nicola S, Palomba M, Pullini D, Horsewell A, Hansen TW et al (2012) Mechanical properties of low density polyethylene filled by graphite nanoplatelets. Nanotechnology 23(48):48705. https://doi.org/10.1088/0957-4484/23/48/485705

Chang C-H, Huang T-C, Peng C-W, Yeh T-C, Lu H-I, Hung W-I, Weng C-J, Yang T-I, Yeh J-M (2012) Novel anti-corrosion coatings prepared from polyaniline/graphene composites. Carbon 50:5044–5051. https://doi.org/10.1016/j.carbon.2012.06.043

Chen X, Fang F, Zhang X, Ding X, Wang Y, Chena L, Tian X (2016) Flame-retardant, electrically conductive and antimicrobial multifunctional coating on cotton fabric via layer-by-layer assembly technique. RSC Adv 6:27669–27676. https://doi.org/10.1039/c5ra26914h

da Silva JEP, Temperini MLA, de Torresi SIC (2005) Characterization of conducting polyaniline blends by resonance raman spectroscopy. J Braz Chem Soc 16(3A):322–327

Daoub RMA, Elmubarak AH, Misran M, Hassan EA, Osman ME (2018) Characterization and functional properties of some natural Acacia gums. J Saudi Soc Agric Sci 17:241–249. https://doi.org/10.1016/j.jssas.2016.05.002

Gao S, Huang J, Li S, Liu H, Li F, Li Y, Chen G, Lai Y (2017) Facile construction of robust fluorine-free superhydrophobic TiO_2@fabrics with excellent anti-fouling, water–oil separation and UV-protective properties. Mater Des 128:1–8. https://doi.org/10.1016/j.matdes.2017.04.091

Hansora DP, Shimpi NG, Mishra S (2015) Graphite to graphene via graphene oxide: an overview on synthesis, properties and applications. J Mater 67(12):2855–2868. https://doi.org/10.1007/s11837-015-1522-5

Hao Y, Tian M, Zhao H, Qu L, Zhu S, Zhang X, Chen S, Wang K, Ran J (2018) High efficiency electrothermal graphene/tourmaline composite fabric joule heater with durable abrasion resistance via a spray coating route. Ind Eng Chem Res 57(40):13437–13448. https://doi.org/10.1021/acs.iecr.8b03628

Hu X, Tian M, Qu L, Zhu S, Han G (2015) Multifunctional cotton fabrics with graphene/polyurethane coatings with far-infrared emission, electrical conductivity and ultraviolet blocking properties. Carbon 95:625–633. https://doi.org/10.1016/j.carbon.2015.08.099

Jain R, Mehrotra R, Mishra S (2019) Synthesis of B doped graphene/polyaniline hybrids for high-performance supercapacitor application. J Mater Sci: Mater Electron 30(3):2316–2326. https://doi.org/10.1007/s10854-018-0504-0

Jeon I-Y, Shin S-H, Choi H-J, Yu S-Y, Jung S-M, Baek J-B (2017) Heavily aluminated graphene nanoplatelets as an efficient flame retardant. Carbon 116:77–83. https://doi.org/10.1016/j.carbon.2017.01.071

Kim H, Abdala AA, Macosko CW (2010) Graphene/polymer nanocomposites. Macromolecules 43:6515–6530. https://doi.org/10.1021/ma100572e

Kuan Y-H, Bhat R, Senan C, Williams PA, Karim AA (2009) Effects of ultraviolet irradiation on the physicochemical and functional properties of gum arabic. J Agric Food Chem 57:9154–9159. https://doi.org/10.1021/jf9015625

Li J, Kim J-K, Sham ML (2005) Conductive graphite nanoplatelet/epoxy nanocomposites:effects of exfoliation and UV/ozone treatment of graphite. Scr Mater 53:235–240

Li Z, Tian M, Sun X, Zhao H, Zhu S, Zhang X (2019) Flexible all-solid planar fibrous cellulose nonwoven fabric-based supercapacitor via capillarity-assisted graphene/MnO_2 assembly. Alloys Compd 782:986–994. https://doi.org/10.1016/j.jallcom.2018.12.254

Liu W, Do I, Fukushima H, Drzal LT (2010) Influence of processing on morphology, electrical conductivity and flexural properties of exfoliated graphite nanoplatelets-polyamide nanocomposites. Carbon Lett 11(4):279–284

Liu L, Huang Z, Pan Y, Wang X, Song L, Hu Y (2018) Finishing of cotton fabrics by multi-layered coatings to improve their flame retardancy and water repellency. Cellulose 25:4791–4803. https://doi.org/10.1007/s10570-018-1866-4

Lu Y, Tian M, Sun X, Pan N, Chen F, Zhu S, Zhang X, Chen S (2019) Highly sensitive wearable 3D piezoresistive pressure sensors based on graphene coated isotropic non-woven substrate. Compos Part A Appl Sci Manuf 117:202–210. https://doi.org/10.1016/j.compositesa.2018.11.023

Mahajan C, Chaudhari P, Mishra S (2018) RGO-MWCNT ZnO based polypyrrole nanocomposites for ammonia gas sensing. J Mater Sci Mater Electron 29:8039–8048. https://doi.org/10.1007/s10854-018-8810-0

Mao H, Wu X, Qian X, An X (2014) Conductivity and flame retardancy of polyaniline-deposited functional cellulosic paper doped with organic sulfonic acids. Cellulose 21:697–704. https://doi.org/10.1007/s10570-013-0122-1

Mishra S, Hansora D (2017) Graphene nanomaterials: fabrication, properties and applications, 1st edn. Pan Stanford, New York, pp 1–100

Montenegro MA, Boiero ML, Valle L, Borsarelli CD (2012) Gum arabic: more than an edible emulsifier. In: Verbeek J (ed) Products and applications of biopolymers. ISBN: 978-953-51-0226-7. http://www.intechopen.com/books/products-and-applications-ofbiopolymers/gum-arabic-more-than-an-edible-emulsifier. Accessed 24 Nov 2018

Nieto A, Lahiri D, Agarwal A (2012) Synthesis and properties of bulk graphene nanoplatelets consolidated by spark plasma sintering. Carbon 50(11):4068–4077. https://doi.org/10.1016/j.carbon.2012.04.054

Nooralian Z, Gashti MP, Ebrahimi I (2016) Fabrication of a multifunctional graphene/polyvinylphosphonic acid/cotton nanocomposite via facile spray layer-by-layer assembly. RSC Adv 6:23288–23299. https://doi.org/10.1039/c6ra00296j

Ozdemir O, Karakuzu R, Sarikanat M, Seki Y, Akar E, Cetin L, Yilmaz OC, Sever K, Sen I, Gurses BO (2015) Improvement of the electromechanical performance of carboxymethylcellulose-based actuators by graphene nanoplatelet loading. Cellulose 22:3251–3260. https://doi.org/10.1007/s10570-015-0702-3

Pandiyarasan V, Archana J, Pavithra A, Ashwin V, Navaneethan M, Hayakawa Y, Ikeda H (2017) Hydrothermal growth of reduced graphene oxide on cotton fabric for enhanced ultraviolet protection applications. Mater Lett 188:123–126. https://doi.org/10.1016/j.matlet.2016.11.047

Qu L, Tian M, Hu X, Wang Y, Zhu S, Guo X, Han G, Zhang X, Sun K, Tang X (2014) Functionalization of cotton fabric at low graphene nanoplate content for ultrastrong ultraviolet blocking. Carbon 80:565–574. https://doi.org/10.1016/j.carbon.2014.08.097

Quintanilha RC, Orth ES, Iankovski AG, Riegel-Vidotti IC, Vidotti M (2014) The use of gum Arabic as Green stabilizer of poly(aniline) nanocomposites: a comprehensive study of spectroscopic, morphological and electrochemical properties. J Colloid Interface Sci 434:18–27. https://doi.org/10.1016/j.jcis.2014.08.006

Sahito IA, Sun KC, Arbab AA, Qadir MB, Jeong SH (2015) Graphene coated cotton fabric as textile structured counter electrode for DSSC. Electrochim Acta 173:164–171. https://doi.org/10.1016/j.electacta.2015.05.035

Sapurina I, Stejskal J (2008) The mechanism of the oxidative polymerization of aniline and the formation of supramolecular polyaniline structures. Polym Int 57:1295–1325

Saville BP (2002) Objective evaluation of fabric handle. In: Woodhead publishing limited (ed.) Physical testing of textiles. CRC, England, pp 258–259

Sen T, Shimpi NG, Mishra S (2016) Room temperature CO sensing by polyaniline/Co_3O_4 nanocomposite. J Appl Polym Sci 133:44115. https://doi.org/10.1002/app.44115

Sen T, Shimpi NG, Mishra S (2017) A β-cyclodextrin based binary dopant for polyaniline: Structural, thermal, electrical, and sensing performance. Mater Sci Eng B 220:13–21. https://doi.org/10.1016/j.mseb.2017.03.003

Sen T, Mishra S, Sonawane SS, Shimpi NG (2018) Polyaniline/zinc oxide nanocomposite as room-temperature sensing layer for methane. Polym Eng Sci 58(8):1438–1445. https://doi.org/10.1002/pen.24740

Šesta E, Dražiča G, Genorioc B, Jermana I (2018) Graphene nanoplatelets as an anticorrosion additive for solar absorber coatings. Solar Energy Mater Solar Cells 176:19–29. https://doi.org/10.1016/j.solmat.2017.11.016

Singh HP, Kaur R, Sekhon SS (2003) Naturally occurring biopolymer as ion conducting material: water uptake, swelling and conductivity studies. Ind Jour of Eng and Mater Sci 10:314–317. http://nopr.niscair.res.in/handle/123456789/24215

Tang X, Tian M, Qua L, Zhu S, Guo X, Han G, Sun K, Hua X, Wang Y, Xu X (2015) Functionalization of cotton fabric with graphene oxide nanosheet and polyaniline for conductive and UV blocking properties. Synth Met 202:82–88. https://doi.org/10.1016/j.synthmet.2015.01.017

Tiwari A (2007) Gum arabic-graft-polyaniline: an electrically active redox biomaterial for sensor applications. J Macromol Sci Part A Pure Appl Chem 44(7):735–745. https://doi.org/10.1080/10601320701353116

Trchová M, Stejskal J (2011) Polyaniline: the infrared spectroscopy of conducting polymer nanotubes (IUPAC technical report). Pure Appl Chem 83:1803–1817. https://doi.org/10.1351/PAC-REP-10-02-01

Trchova M, Sÿedenkova I, Konyushenko EN, Stejskal J, Holler P, Marjanovic GC (2006) Evolution of polyaniline nanotubes: the oxidation of aniline in water. J Phys Chem B 110:9461–9468. https://doi.org/10.1021/jp057528g

Yang QC, Wei W, Lickfield GC (2000) Mechanical strength of durable press finished cotton fabric part III: change in cellulose molecular weight. Text Res J 70(10):910–915. https://doi.org/10.1177/004051750007001010

Yasmin A, Daniel IM (2004) Mechanical and thermal properties of graphite platelet/epoxy composites. Polymer 45:8211–8219. https://doi.org/10.1016/j.polymer.2004.09.054

Yu J, Zhou T, Pang Z, Wei Q (2015) Flame retardancy and conductive properties of polyester fabrics coated with polyaniline. Text Res J 86(11):1171–1179. https://doi.org/10.1177/0040517515606360

Zhang L, Peng H, Zujovic ZD, Kilmartin PA, Travas-Sejdic J (2007) Characterization of polyaniline nanotubes formed in the presence of amino acids. Macromol Chem Phys 208:1210–1217. https://doi.org/10.1002/macp.200700013

Zhang C, Zhong L, Wang D, Zhang F, Zhang G (2018a) Anti-ultraviolet and anti-static modification of polyethylene terephthalate fabrics with graphene nanoplatelets by a high temperature and high-pressure inlaying method. Text Res J. https://doi.org/10.1177/0040517518773375

Zhang F, Gao W, Jia Y, Lu Y, Zhang G (2018b) A concise water-solvent synthesis of highly effective, durable, and eco-friendly flame-retardant coating on cotton fabrics.

Carbohydr Polym 199:256–265. https://doi.org/10.1016/j.carbpol.2018.05.085

Zhao H, Tian M, Li Z, Zhang Y, Zhu S, Zhang X, Chen S, Qu L (2019) Enhanced electrical conductivity of silver nanoparticles decorated fabrics with sandwich microstructure coating layer based on silver colloid effect. Mater Lett 240:5–8. https://doi.org/10.1016/j.matlet.2018.12.052